Supporting Information

Controlled Growth of Large-Area Bilayer Tungsten Diselenides with Lateral *P-N* Junctions

Srinivas V. Mandyam,[⊥,†] Meng-Qiang Zhao,[⊥,†] Paul Masih Das,[†] Qicheng Zhang,[†] Christopher C. Price,[§] Zhaoli Gao,[†] Vivek B. Shenoy,[§] Marija Drndić,[†] Alan T. Charlie Johnson[†,]*

[†] Department of Physics and Astronomy, University of Pennsylvania, 209 South 33rd Street, Philadelphia, PA 19104, USA

[§] Department of Materials Science and Engineering, University of Pennsylvania, 3231 Walnut St., Philadelphia, PA 19104, USA

AUTHOR INFORMATION

[⊥] These authors contribute equally to this work.

Corresponding Author

*Email: cjohnson@physics.upenn.edu

SUPPLEMENTARY FIGURES

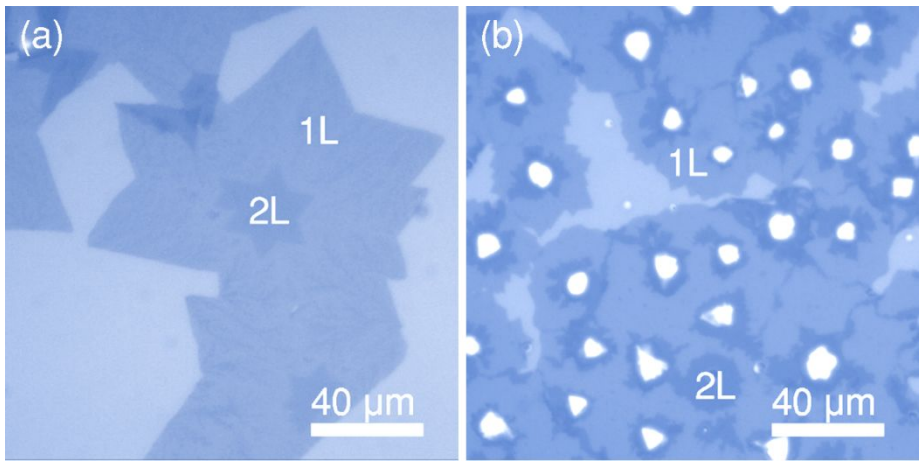

Figure S1. Optical images of the as-grown WSe_2 flakes using (a) 25 mM $C_{24}H_{40}NaO_5$ + 125 mM NaCl and (b) 25 mM $C_{24}H_{40}NaO_5$ + 500 mM NaCl as the growth promoter. The bright spots in (b) are multilayer WSe_2.

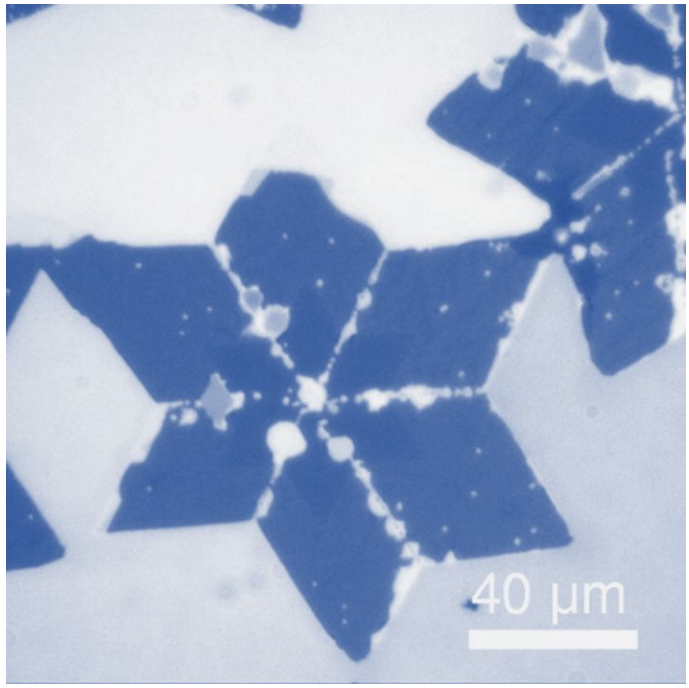

Figure S2. Optical image of a partially oxidized bilayer WSe_2 flake, in which the grain boundaries are clearly observed.

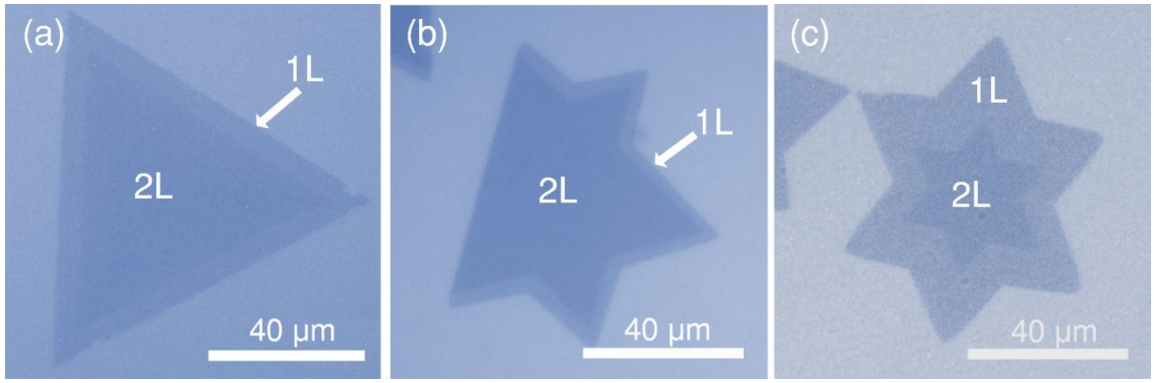

Figure S3. Optical images of bilayer WSe_2 flakes with varied morphologies using a mixture of 25 mM $C_{24}H_{40}NaO_5$ and 250 mM NaCl as the growth promoter.

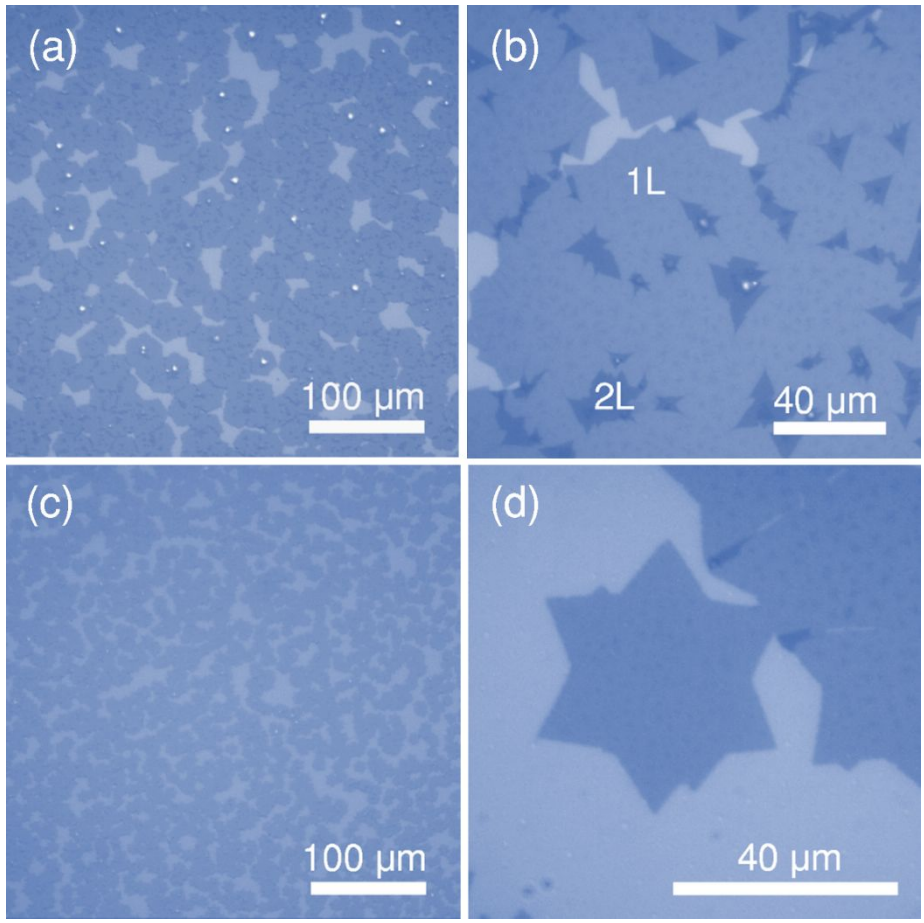

Figure S4. Optical images of the as-grown WSe_2 flakes using (a,b) 75 mM NaCl and (c,d) 25 mM NaCl as the growth promoter.

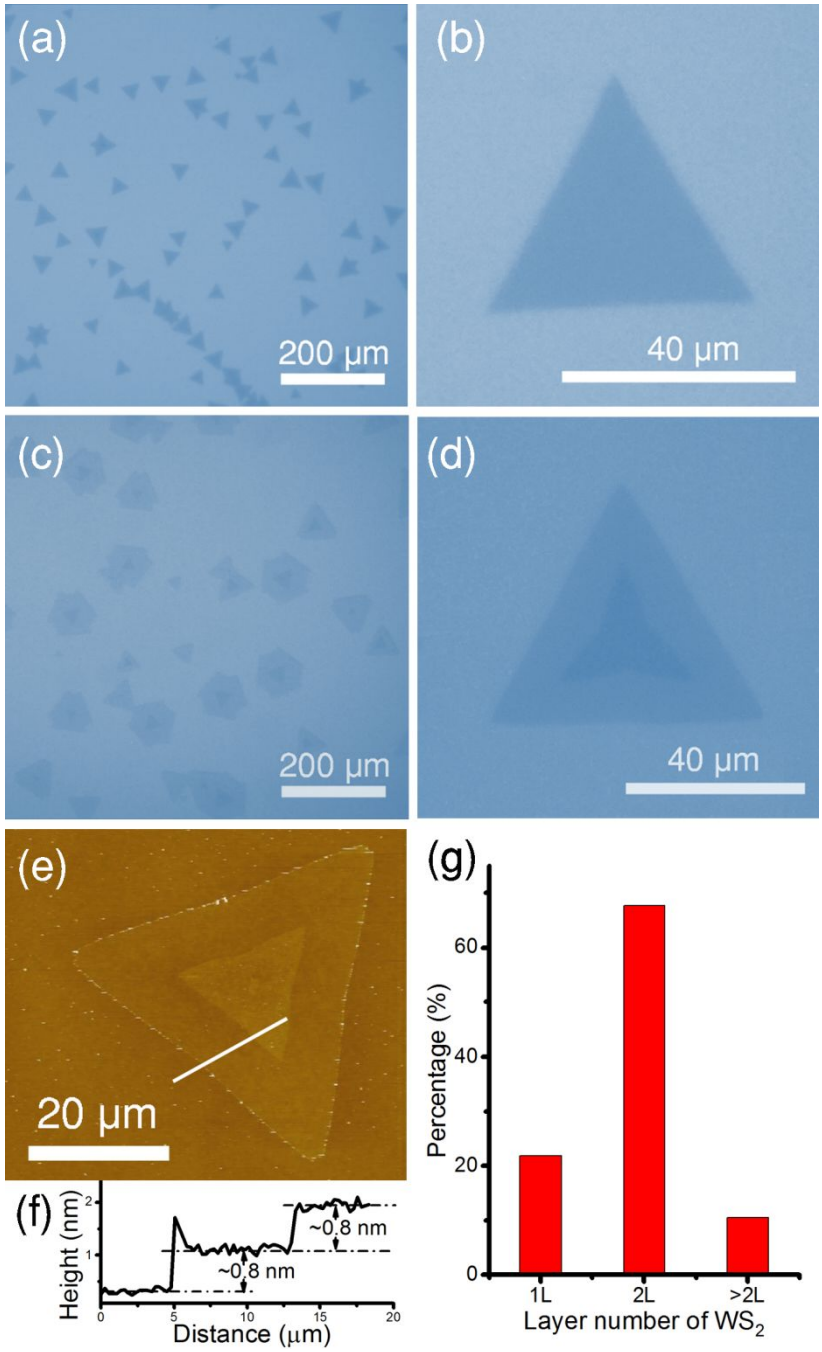

Figure S5. Optical images of WS_2 flakes grown by CVD using (a,b) 25 mM $C_{24}H_{40}NaO_5$ and (c,d) 25 mM $C_{24}H_{40}NaO_5$ and 250 mM NaCl as the growth promoter. (e) Atomic force microscope image of a bilayer WS_2 flake and (f) corresponding height profile; (g) Statistical analysis on the layer number of WS_2 flakes grown using 25 mM $C_{24}H_{40}NaO_5$ and 250 mM NaCl as the growth promoter, showing the preferential growth of bilayer material.

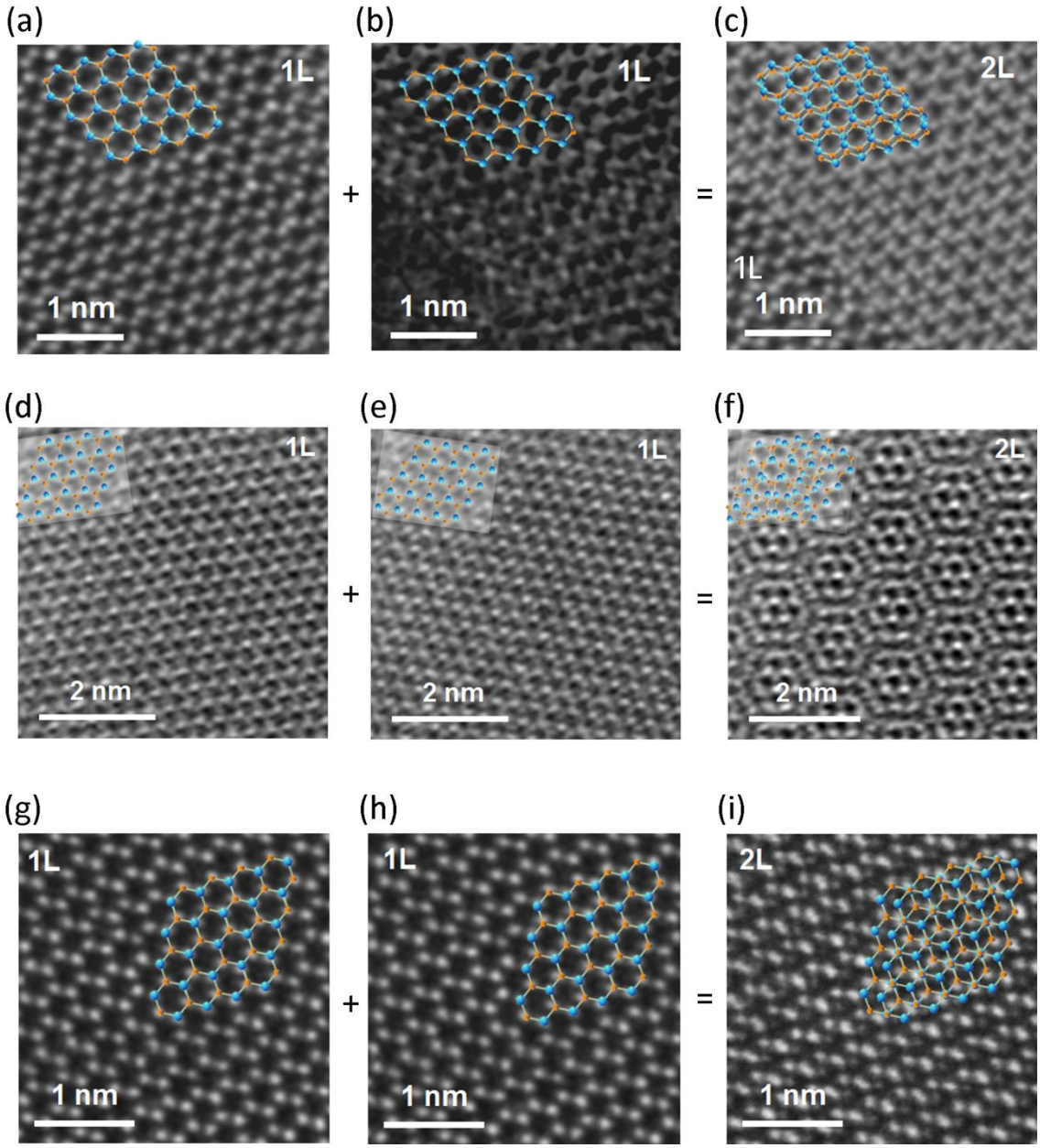

Figure S6. Analysis of the stacking orientation and atomic structure of bilayer WSe_2 by fast Fourier transform (FFT) decomposition of the 2L regions: (a-c) 60° twist angle or AA' stacking; (d-f) 15° twist angle; (g-i) 0° twist angle or AB stacking. In each set of the 3 images, the 2L regions is decomposed into two monolayers by FFT to identify the corresponding atomic models. The related inset images present the corresponding atomic models.

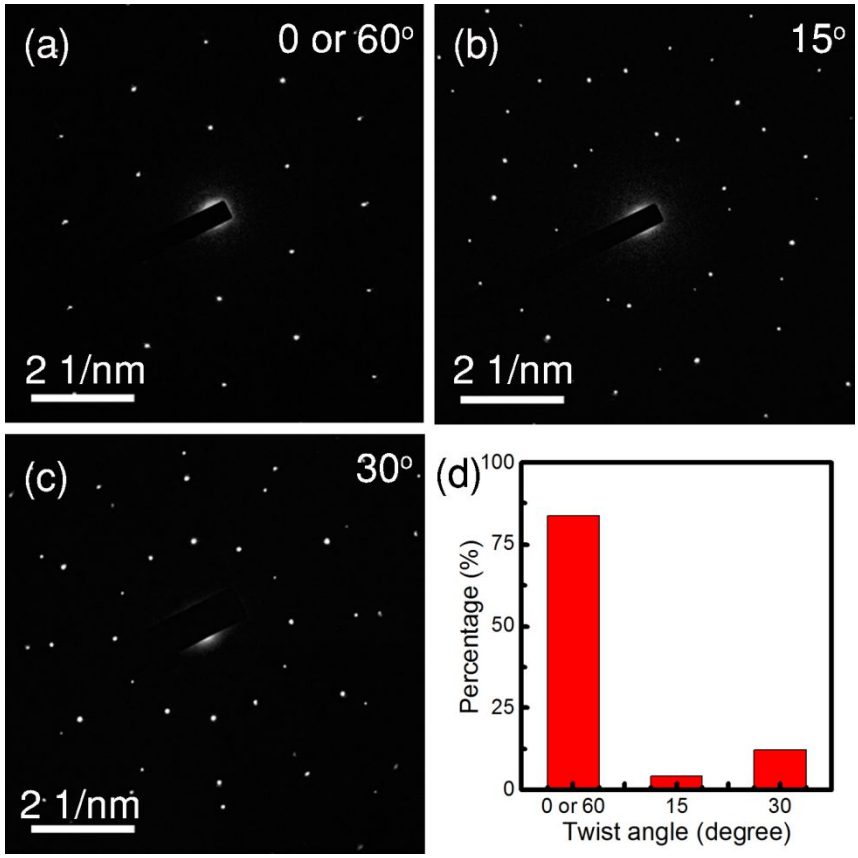

Figure S7. Selected area electron diffraction (SAED) patterns of bilayer WSe_2 flakes with (a) 0 or 60° twist, (b) 15° and (c) 30° twist angles; (d) Histogram of twist angle frequencies based on ~100 bilayer WSe_2 flakes.

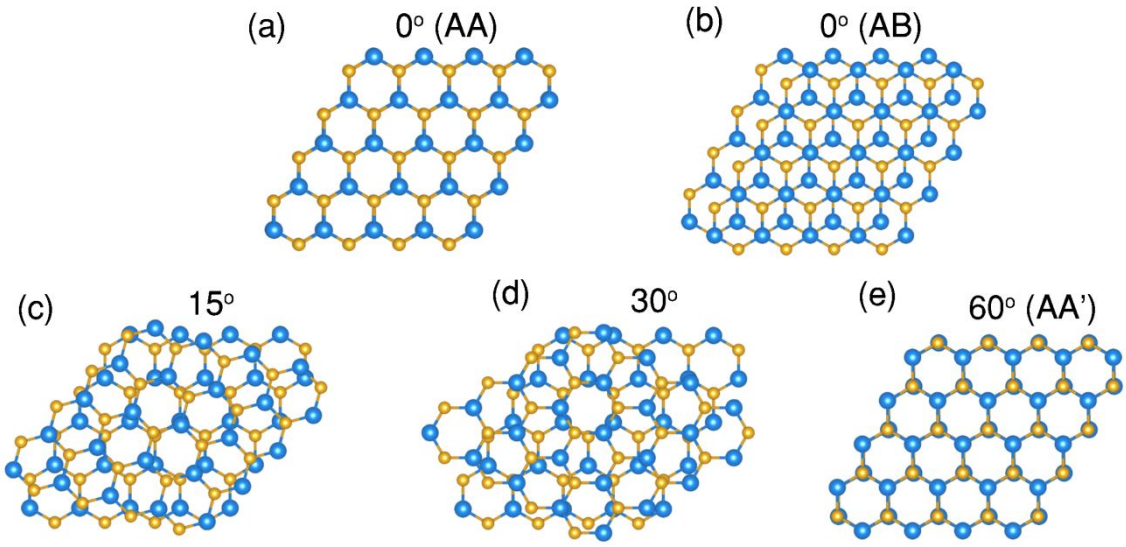

Figure S8. Summary of the atomic models of bilayer WSe_2 with varied stacking orientations.

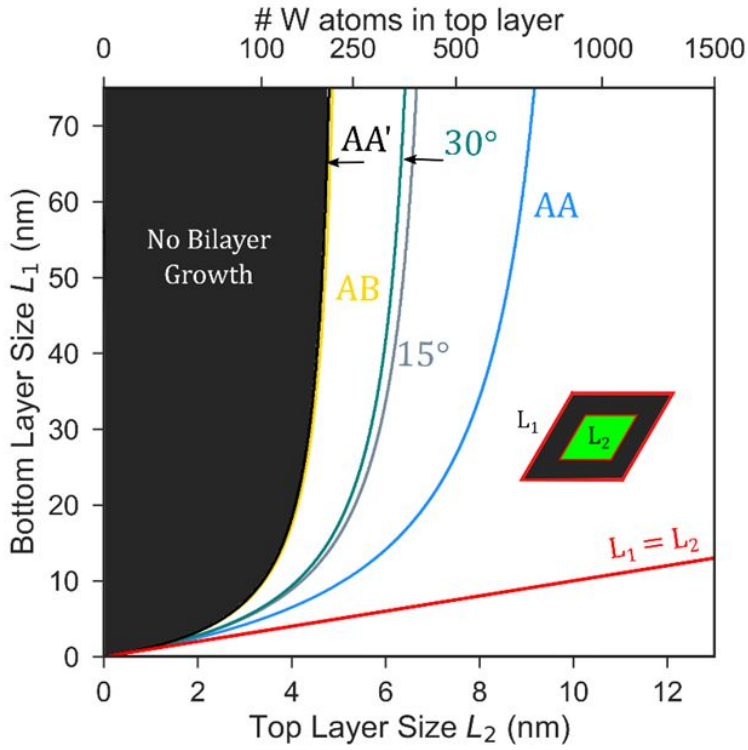

Figure S9. Thermodynamic growth diagram for bilayer WSe_2 flakes as a function of the instantaneous layer sizes L1 (bottom layer) and L2 (top layer). The lines mark the minimum required top layer size for thermodynamically favorable bilayer growth of triangular flakes over the range of bottom layer sizes.

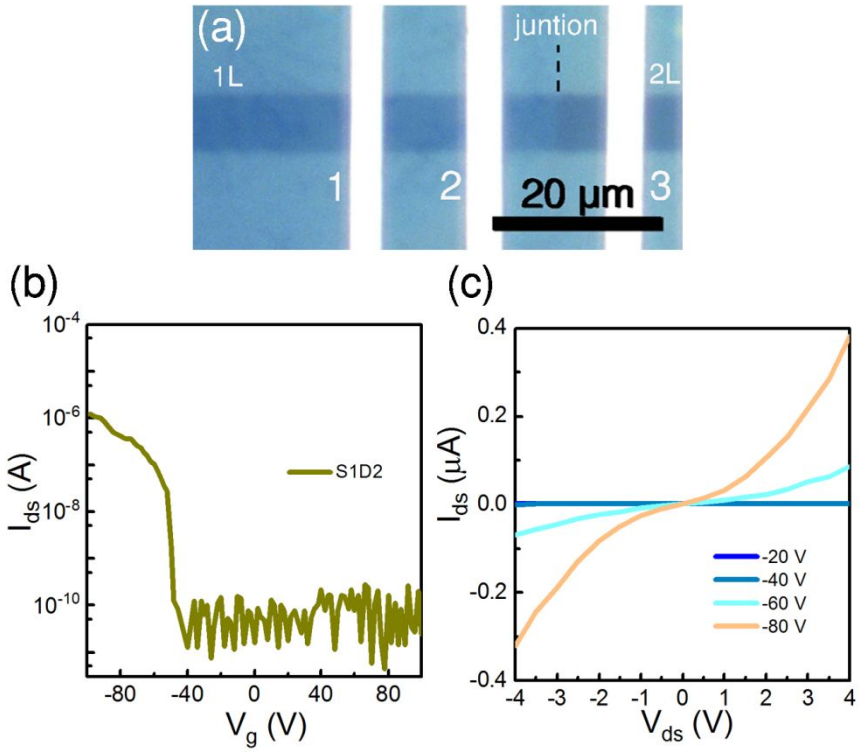

Figure S10. (a) Optical micrograph of a device structure based on a bilayer flake containing a large monolayer region. The electrode pair S1D2 contacts the monolayer region. (b) I_{ds}-V_g curves for the S1D2 FET device. (c) I_{ds}-V_{ds} curves for the WSe_2-based FET at different values of the backgate voltage.